Aryl hydrocarbon receptor is essential for the pathogenesis of pulmonary arterial hypertension

Takeshi Masaki[a,b,1], Makoto Okazawa[a,1], Ryotaro Asano[c,d], Tadakatsu Inagaki[a], Tomohiko Ishibashi[a], Akiko Yamagishi[a], Saori Umeki-Mizushima[a], Manami Nishimura[a], Yusuke Manabe[a,e], Hatsue Ishibashi-Ueda[f], Manabu Shirai[g], Hirotsugu Tsuchimochi[h], James T Pearson[h], Atsushi Kumanogoh[e], Yasushi Sakata[b], Takeshi Ogo[c,d], Tadamitsu Kishimoto[i,2], and Yoshikazu Nakaoka[a,b,2]

[a]Department of Vascular Physiology, National Cerebral and Cardiovascular Center Research Institute, 564-8565 Suita, Japan; [b]Department of Cardiovascular Medicine, Osaka University Graduate School of Medicine, 565-0871 Suita, Japan; [c]Department of Advanced Medical Research for Pulmonary Hypertension, National Cerebral and Cardiovascular Center, 564-8565 Suita, Japan; [d]Department of Cardiovascular Medicine, National Cerebral and Cardiovascular Center, 564-8565 Suita, Japan; [e]Department of Respiratory Medicine and Clinical Immunology, Osaka University Graduate School of Medicine, 565-0871 Suita, Japan; [f]Department of Pathology, National Cerebral and Cardiovascular Center, 564-8565 Suita, Japan; [g]Omics Research Center, National Cerebral and Cardiovascular Center, 564-8565 Suita, Japan; [h]Department of Cardiac Physiology, National Cerebral and Cardiovascular Center Research Institute, 564-8565 Suita, Japan; and [i]Department of Immune Regulation, Immunology Frontier Research Center, Osaka University, 565-0871 Suita, Japan

Contributed by Tadamitsu Kishimoto, January 22, 2021 (sent for review November 19, 2020; reviewed by Christopher A. Bradfield and Tak W. Mak)

Pulmonary arterial hypertension (PAH) is a devastating disease characterized by arteriopathy in the small to medium-sized distal pulmonary arteries, often accompanied by infiltration of inflammatory cells. Aryl hydrocarbon receptor (AHR), a nuclear receptor/transcription factor, detoxifies xenobiotics and regulates the differentiation and function of various immune cells. However, the role of AHR in the pathogenesis of PAH is largely unknown. Here, we explore the role of AHR in the pathogenesis of PAH. AHR agonistic activity in serum was significantly higher in PAH patients than in healthy volunteers and was associated with poor prognosis of PAH. Sprague–Dawley rats treated with the potent endogenous AHR agonist, 6-formylindolo[3,2-b]carbazole, in combination with hypoxia develop severe pulmonary hypertension (PH) with plexiform-like lesions, whereas Sprague–Dawley rats treated with the potent vascular endothelial growth factor receptor 2 inhibitors did not. *Ahr*-knockout ($Ahr^{-/-}$) rats generated using the CRISPR/Cas9 system did not develop PH in the SU5416/hypoxia model. A diet containing Qing-Dai, a Chinese herbal drug, in combination with hypoxia led to development of PH in $Ahr^{+/+}$ rats, but not in $Ahr^{-/-}$ rats. RNA-seq analysis, chromatin immunoprecipitation (ChIP)-seq analysis, immunohistochemical analysis, and bone marrow transplantation experiments show that activation of several inflammatory signaling pathways was up-regulated in endothelial cells and peripheral blood mononuclear cells, which led to infiltration of $CD4^+$ IL-21^+ T cells and $MRC1^+$ macrophages into vascular lesions in an AHR-dependent manner. Taken together, AHR plays crucial roles in the development and progression of PAH, and the AHR-signaling pathway represents a promising therapeutic target for PAH.

pulmonary arterial hypertension | inflammation | transcription factor | aryl hydrocarbon receptor (AHR) | Qing-Dai

Pulmonary arterial hypertension (PAH) is a devastating disease characterized by arteriopathy in the small to medium-sized distal pulmonary arteries that are associated with arterial muscularization and formation of plexiform lesions (1, 2). The pathogenesis of PAH may be influenced by external and internal environmental factors including infections, diet, drugs, pollutants, and homeostatic imbalances, as well as genetic background, epigenetic factors, and preexisting diseases (3, 4). Immune responses, which can be activated by both external and internal environmental factors, contribute to vascular diseases such as arteriosclerosis (5), vasculitis (6, 7) and PAH (8), as well as to host defense, allergy, and autoimmune disease (9, 10). Multiple inflammatory signaling molecules are elevated in patients with PAH and in PAH model animals (11–13). Interleukin (IL)-6, tumor necrosis factor (TNF)α, and IL-1β have been implicated in human PAH prognosis (8). However, the causal relationship between environmental factors and the pathogenic mechanism of PAH via inflammatory signaling is still elusive.

Aryl hydrocarbon receptor (AHR), a nuclear receptor/transcription factor, detoxifies xenobiotics (14, 15) and regulates various immune-related diseases by controlling inflammatory signals, including cytokine and chemokine signals (16–19). The SU5416/hypoxia (SuHx) rat model is widely used because it reproduces many features of severe PAH, such as intimal and plexiform lesions (20, 21). Inhibition of vascular endothelial growth factor receptor 2 (VEGFR2) by SU5416 has been postulated to contribute to the pathogenesis of PAH (20–22); however, the inhibitory potency of this compound is low at micromolar concentrations (23). By contrast, SU5416 is a potent activator of AHR both in vivo and in vitro and exerts these effects at subnanomolar concentrations (24). The strong effect of SU5416 for AHR agonistic activity suggests that pathogenesis of

Significance

Inflammatory signals are thought to be crucial for the pathogenesis of PAH; however, the underlying mechanism is still largely unknown. In this study, we demonstrate that AHR makes a causal contribution to the pathogenesis of PAH, activating a focal inflammatory response in the lungs and promoting infiltration of immune cells from the bone marrow. Furthermore, we found that PAH patients with higher AHR agonistic activity in sera are more susceptible to severe clinical events than those with lower activity. Because conventional therapy for pulmonary hypertension targeting pulmonary artery vasodilation has limited efficacy against severe PAH, the AHR-signaling pathway represents a promising therapeutic target for PAH. In addition, AHR agonistic activity in serum represents a biomarker for PAH.

Author contributions: T.M., M.O., T. Inagaki, T. Ishibashi, T.K., and Y.N. designed research; T.M., M.O., R.A., T. Inagaki, T. Ishibashi, A.Y., S.U.-M., M.N., Y.M., H.I.-U., M.S., T.O., and Y.N. performed research; T.M., M.O., T. Inagaki, T. Ishibashi, A.Y., H.I.-U., M.S., H.T., J.T.P., A.K., Y.S., T.O., and Y.N. analyzed data; and T.M., M.O., and Y.N. wrote the paper.

Reviewers: C.A.B., University of Wisconsin, Madison; and T.W.M., University of Toronto.

Competing interest statement: R.A. and T.O. belong to a department endowed by funding from Nippon Shinyaku Co., Ltd.

[1]T.M. and M.O. contributed equally to this work.

[2]To whom correspondence may be addressed. Email: kishimoto@ifrec.osaka-u.ac.jp or ynakaoka@ncvc.go.jp.

This article contains supporting information online at https://www.pnas.org/lookup/suppl/doi:10.1073/pnas.2023899118/-/DCSupplemental.

Published March 8, 2021.

PAH in the SuHx model may also involve activation of AHR as well as inhibition of VEGFR2 (25, 26). We previously reported that the IL-6/Th17 (T helper 17)/IL-21 axis plays a crucial role in a hypoxia-induced pulmonary hypertension (HPH) model in mouse (13) and demonstrated that IL-6 is a critical cytokine for Th17 cell differentiation (27) through induction of AHR expression in naive T cells (28, 29). Therefore, AHR, along with IL-6, might be a key regulator of the pathogenesis of PAH.

Several recent studies have described the adverse events of drug-induced PAH in patients with ulcerative colitis (UC) treated with the Chinese herbal medicine Qing-Dai (30–32), which contains abundant AHR agonists (33). Therefore, we hypothesized that AHR is also involved in the pathogenesis of Qing-Dai–induced PAH. Here, we investigated the roles of AHR in the development and progression of PAH using both rat pulmonary hypertension (PH) models and human specimens.

Results

AHR-Luc Activity of Serum Depicts the Progression of PAH. AHR translocates from the cytoplasm to the nucleus after binding to its agonist and activates the transcription of its target genes (*SI Appendix*, Fig. S1*A*). To explore the involvement of AHR in the pathogenesis of PAH in humans, we performed AHR luciferase reporter assay using the sera of PAH patients and healthy volunteers (HV). AHR agonistic (AHR-Luc) activity was significantly higher in patients with PAH than in HV (Fig. 1*A*). Interestingly, AHR-Luc activity was significantly greater in patients with severe PAH (World Health Organization [WHO] functional class 3 and 4) than in those with mild PAH (WHO functional class 1 and 2) (Fig. 1*B*). Furthermore, patients with higher AHR-Luc activity were significantly more susceptible to severe clinical events such as death, lung transplantation, or hospitalization for right heart failure than those with lower activity (Fig. 1*C*). The relationship between AHR-Luc activity in the sera from PAH patients and clinical prognosis suggests that AHR activation plays an essential role in the pathogenesis of PAH.

Administration of the Endogenous AHR Agonist FICZ Induces Severe PH with Plexiform-like Lesions. To confirm the causal relationship between AHR activation and PAH pathogenesis, we examined the effects of AHR agonists on rat lungs. Subcutaneous administration of 6-formylindolo[3,2-b]carbazole (FICZ), an endogenous potent AHR agonist (*SI Appendix*, Fig. S1*B*), to rats under normoxic conditions (*SI Appendix*, Fig. S1*C*) induced mild to severe elevation of right ventricular systolic pressure (RVSP) and Fulton's index in most rats (*SI Appendix*, Fig. S1 *D* and *E*). Occlusive neointimal lesions were observed in small arteries and distal acinar arterioles of these PH rats (*SI Appendix*, Fig. S1*F*), indicating that AHR activation might lead to the development of a severe PAH phenotype. Administration of FICZ along with hypoxia exposure during the first 3 wk of the experiment (FICZ/hypoxia/normoxia: FICZ/Hx/Nx rat model; Fig. 2*A* and *SI Appendix*, Fig. S1*G*) induced marked elevation of RVSP (Fig. 2*B*) and Fulton's index (Fig. 2*C*). The distal acinar arterioles of FICZ/Hx/Nx rats exhibited both medial wall thickening (Fig. 2 *D* and *E*) and occlusive neointimal lesions (Fig. 2 *D*, *F*, and *G*) with plexiform-like lesions (*SI Appendix*, Fig. S1*H*). Since the inhibition of VEGFR2 is thought to be responsible for the induction of severe PH including the most widely used SuHx rat model (21), we examined effects of VEGFR2 inhibition of FICZ. FICZ did not suppress VEGFR2 phosphorylation by VEGFA (Fig. 3*A*). These results indicate that AHR activation is essential for the development and progression of PAH.

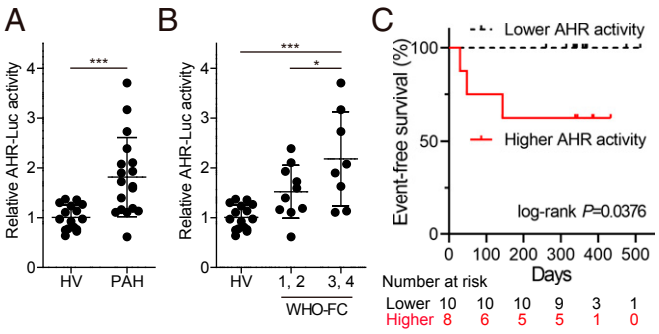

Fig. 1. AHR agonistic activity in sera is up-regulated in the patients with PAH and reflects PAH severity. (*A*) AHR-Luc activity in sera from HV and PAH patients, determined by AHR luciferase reporter assay (HV: $n = 16$, PAH: $n = 18$). (*B*) Distribution of AHR-Luc activity classified by WHO functional class (WHO-FC) (HV: $n = 16$; WHO-FC 1, 2: $n = 10$; WHO-FC 3, 4: $n = 8$). (*C*) Kaplan–Meier analysis of event-free survival of patients with lower AHR-Luc activity ($n = 10$) or higher AHR-Luc activity ($n = 8$) ($P = 0.0376$, two-sided log-rank test). The major clinical events were defined as death, lung transplantation, and hospitalization for right heart failure. Values are means ± SD; $***P < 0.001$, $*P < 0.05$.

Inhibition of VEGFR2 Does Not Induce PH Even in Combination with Hypoxia. To determine the contribution of VEGFR2 inhibition on the pathogenesis of PH, we administered VEGFR2 inhibitors with AHR agonistic activity (SU5416) or without AHR agonistic activity [Ki8751 (34) and TAK-593 (35)] (Fig. 3*A* and *SI Appendix*, Fig. S1*B*) into rats and exposed them to chronic hypoxia (Fig. 3*B*). In contrast to SU5416, neither Ki8751 nor TAK-593 up-regulated RVSP (Fig. 3*C*), Fulton's index (Fig. 3*D*), and pulmonary arterial remodeling (Fig. 3 *E*–*H*), even in combination with hypoxia. These findings strongly suggest that inhibition of VEGFR2 is dispensable for the pathogenesis of PH.

AHR Is a Critical Driver of the Pathogenesis of PH. To confirm the importance of AHR in the pathogenesis of PH, we generated $Ahr^{-/-}$ rats (*SI Appendix*, Fig. S2*A*) using CRISPR/Cas9 gene editing. As in the previous study (36), $Ahr^{-/-}$ rats showed renal pathological alteration and had normal characteristics in kidney and liver function assessed by serum biochemical test (*SI Appendix*, Fig. S2 *B*–*K*). In the FICZ/Hx/Nx model (*SI Appendix*, Fig. S3*A*), PH phenotypes were suppressed in $Ahr^{-/-}$ rats (*SI Appendix*, Fig. S3 *B* and *C*). We next examined the effect of AHR deletion on the PH phenotypes in the SuHx rat PH model (Fig. 4*A*). $Ahr^{-/-}$ rats did not exhibit elevation of either RVSP (Fig. 4*B*) or Fulton's index (Fig. 4*C*). The medial wall thickness index of intraacinar arterioles was considerably lower in $Ahr^{-/-}$ rats than in $Ahr^{+/+}$ rats (Fig. 4 *D* and *E*). No closed arterioles of intraacinar arteries were observed in $Ahr^{-/-}$ rats (Fig. 4 *D*, *F*, and *G*). $Ahr^{-/-}$ female rats also showed resistance to SuHx PH (*SI Appendix*, Fig. S3 *D*–*F*). These findings indicate that AHR plays an essential role in the pathogenesis of PAH. Interestingly, in the lungs of SuHx rats, RVSP and Fulton's index were positively correlated with messenger RNA (mRNA) levels of *Cyp1a1*, a typical gene whose expression is directly up-regulated by AHR (Fig. 4 *H* and *I*).

AHR Plays Essential Roles in the Pathogenesis of Qing-Dai–Induced PAH. To examine the involvement of AHR in Qing-Dai–induced PAH, we fed rats a Qing-Dai–containing diet or control diet for 5 wk; the rats were also exposed to hypoxia during the first 3 wk (Fig. 5*A*). In the Qing-Dai group, both RVSP and Fulton's index were higher than in the normal diet group (Fig. 5 *B* and *C*), indicating that the phenotype of Qing-Dai–induced PAH was recapitulated in the rats. Next, we challenged $Ahr^{-/-}$ rats and their littermates with a Qing-Dai–containing diet with 3 wk of hypoxia and 2 wk of normoxia (Fig. 5*D*). RVSP and Fulton's index of $Ahr^{-/-}$ rats were significantly lower than those of $Ahr^{+/+}$ rats, respectively (Fig. 5 *E* and *F*). These findings indicate that AHR is responsible for the development of Qing-Dai–induced PAH.

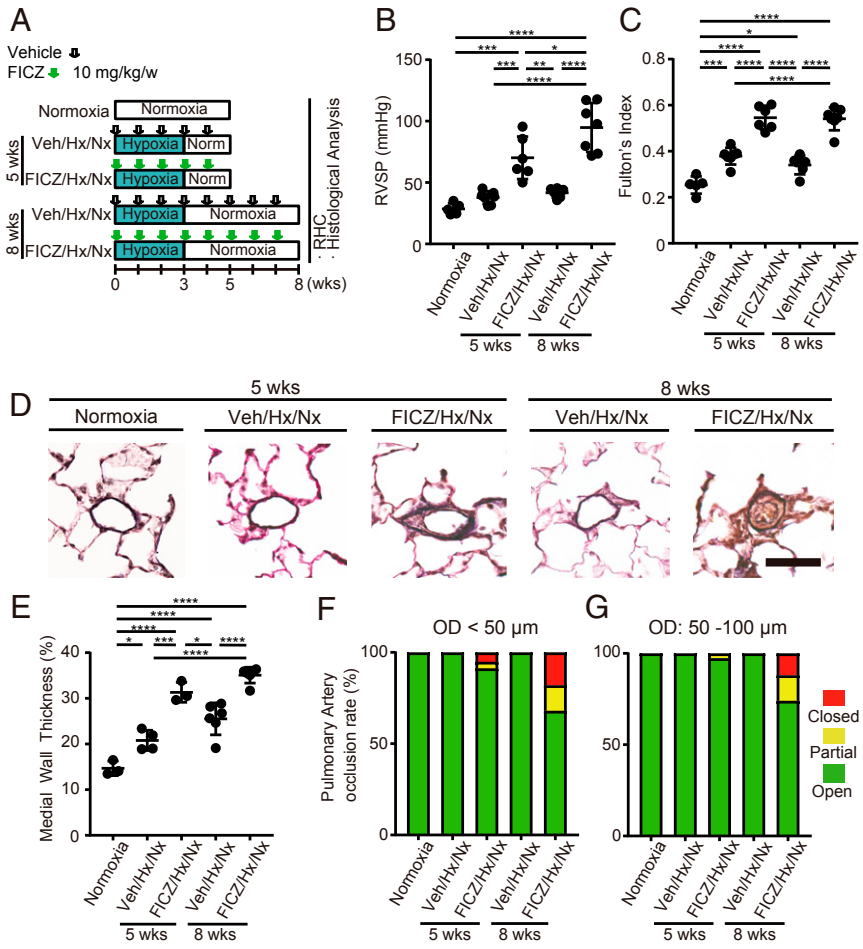

Fig. 2. The endogenous AHR ligand FICZ induces severe PH in rats in combination with hypoxia. (*A*) Experimental protocol for determining whether FICZ treatment can induce PH in rats in combination with hypoxia (FICZ/Hx/Nx model). FICZ or vehicle was subcutaneously administered to rats every week. The rats were housed in a state of hypoxia (10% oxygen) for the first 3 wk, followed by normoxia for 2 or 5 wk. RHC: right heart catheterization. (*B* and *C*) Assessment of FICZ/Hx/Nx rats (Veh: vehicle, Hx: hypoxia, Nx: normoxia; normoxia: $n = 5$, Veh/Hx/Nx 5 wk: $n = 7$, FICZ/Hx/Nx 5 wk: $n = 6$, Veh/Hx/Nx 8 wk: $n = 6$, FICZ/Hx/Nx 8 wk: $n = 7$). RVSP (*B*), Fulton's index (*C*). (*D*) Representative images of the vascular remodeling of distal acinar arterioles in lung sections subjected to Elastica van Gieson (EVG) staining in normoxia, Veh/Hx/Nx 5-wk, FICZ/Hx/Nx 5-wk, Veh/Hx/Nx 8-wk, and FICZ/Hx/Nx 8-wk rats. (Scale bar, 30 μm.) (*E*) Medial wall thickness index of FICZ/Hx/Nx rats (normoxia: $n = 3$, Veh/Hx/Nx 5 wk: $n = 4$, FICZ/Hx/Nx 5 wk: $n = 3$, Veh/Hx/Nx 8 wk: $n = 6$, FICZ/Hx/Nx 8 wk: $n = 6$). (*F* and *G*) Pulmonary arterial occlusions were graded as open (no luminal occlusion; green), partial (<50% occlusion; yellow), or closed (≥50% occlusion; red). Percentages of open, partial, and closed pulmonary arteries of outer diameter (OD) < 50 μm (*F*) and OD: 50–100 μm (*G*) in FICZ/Hx/Nx rats (normoxia: $n = 3$, Veh/Hx/Nx 5 wk: $n = 4$, FICZ/Hx/Nx 5 wk: $n = 3$, Veh/Hx/Nx 8 wk: $n = 6$, FICZ/Hx/Nx 8 wk: $n = 6$). Values are means ± SD; $^{****}P < 0.0001$, $^{***}P < 0.001$, $^{**}P < 0.01$, $^{*}P < 0.05$.

Administration of indirubin, a major component of Qing-Dai, along with hypoxia exposure (Fig. 5*G*) also induced up-regulation of RVSP (Fig. 5*H*) and a trend toward increased Fulton's index (Fig. 5*I*). Those PH phenotypes induced by indirubin administration were abolished in $Ahr^{-/-}$ rats (Fig. 5 *J*–*L*). These results suggest that indirubin is one of the causative compounds of Qing-Dai–induced PAH.

Inflammatory Signals Are Activated in SuHx Lungs through Activation of Endothelial AHR. To understand the acutely regulated genes by AHR in the lungs of SuHx rats, we performed RNA-seq analysis on day 4 (Fig. 6*A*), the initial stage of the model. We also performed chromatin immunoprecipitation (ChIP)-seq on days 0, 4, and 8 wk (Fig. 6*B*). In addition to representative AHR-downstream genes such as *Cyp1a1*, several PAH-related genes were significantly up- or down-regulated in SuHx $Ahr^{-/-}$ rats (Fig. 6*C*). Gene set enrichment analysis (GSEA) revealed that genes involved in chemokine secretion were enriched in $Ahr^{+/+}$ SuHx rats (Fig. 6*D*). Many inflammation-related genes, including *Tlr5, Ptx3, Ackr3, Il1r1, C1qa, C1qb, C1qc, Cxcl10,* and *Edn1,* were up-regulated in an AHR-dependent manner (Fig. 6 *E*, *Upper*). In addition, ChIP-seq analysis revealed that many of these genes were directly regulated by AHR (Fig. 6 *E*, *Lower*). Peaks of AHR binding in SuHx lungs were mainly located in promoter regions (29.0%) and introns (26.3%) (Fig. 6*F*). Because AHR activation was observed mainly in endothelial cells (ECs) of the lung on day 4 (Fig. 6 *G* and *H*), we focused on endothelium-specific genes (Fig. 6*I*). Sixty of 168 AHR-dependently up-regulated genes (or genes down-regulated in $Ahr^{-/-}$) and 54 of 210 AHR-dependently down-regulated genes (or genes up-regulated in $Ahr^{-/-}$) were detected in ECs (Fig. 6 *J* and *K*). Interestingly, some of these genes were related to PAH (Fig. 6 *J* and *K*). Gene ontology (GO) enrichment analysis using the 60 genes up-regulated in ECs and down-regulated in $Ahr^{-/-}$ revealed up-regulation of several inflammation-associated biological processes (i.e., chemokine-mediated signaling pathway, inflammatory response, and cellular response to IL-1) (Fig. 6*L*).

AHR Induces Up-Regulation of Inflammatory Signals and Accumulation of $CD4^{+}IL\text{-}21^{+}$ T Cells in Vascular Lesions in the Advanced Stage of SuHx Rats. To elucidate the mechanisms underlying the AHR-dependent development of severe PH phenotypes including intimal and plexiform-like

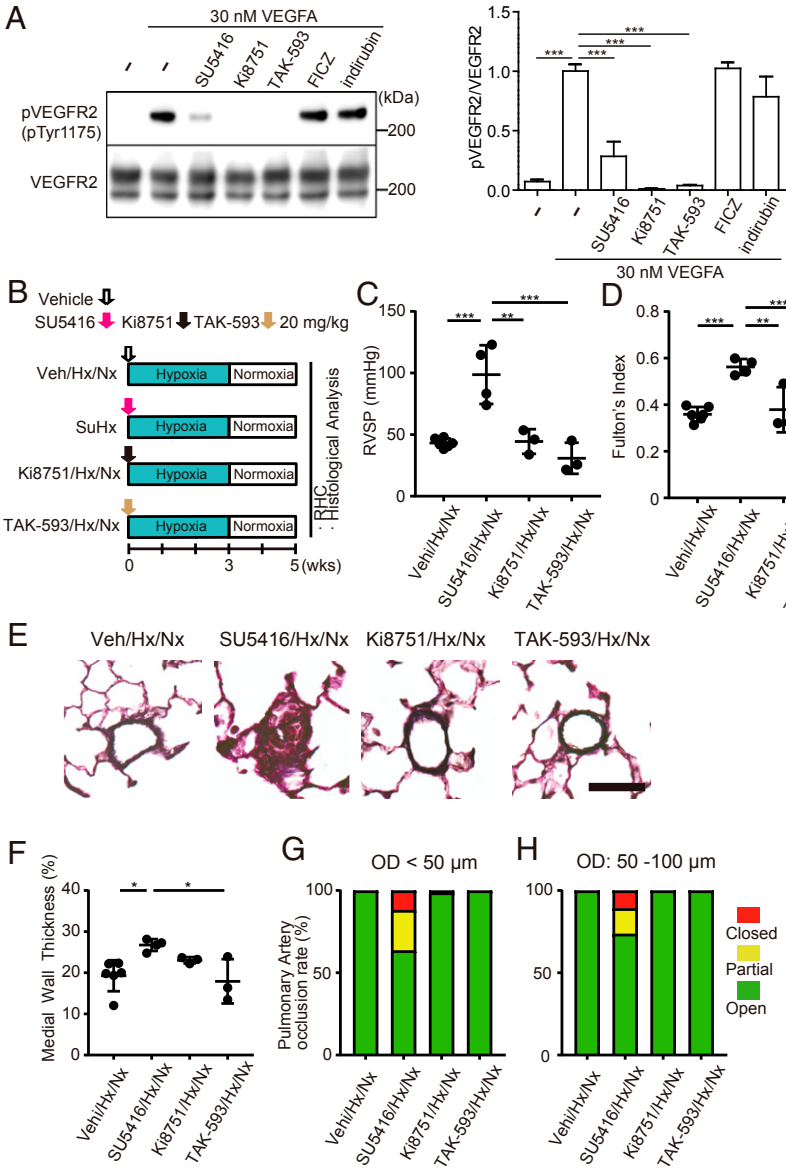

Fig. 3. Potent VEGFR2 inhibitors do not induce PH in rats even in combination with hypoxia. (*A*) Western blotting of pVEGFR2 and total VEGFR2 (*Left*) and quantification of pVEGFR2 (*Right*). SU5416, Ki8751, and TAK-593, but not FICZ and indirubin, inhibited phosphorylation of VEGFR2 by VEGFA. (*B*) Experimental protocol for comparing the effect of Ki8751 and TAK-593 treatment with that of SU5416, in combination with hypoxia in rats. SU5416, Ki8751, TAK-593, or vehicle was subcutaneously administered once on day 0. (*C* and *D*) Assessment of SuHx, Ki8751/Hx/Nx, and TAK-593/Hx/Nx rats (Veh/Hx/Nx: $n = 6$, SuHx: $n = 4$, Ki8751/Hx/Nx: $n = 3$, TAK-593/Hx/Nx: $n = 3$). RVSP (*C*), Fulton's index (*D*). (*E*) Representative images of distal acinar arterioles in lung sections of SuHx, Ki8751/Hx/Nx, or TAK-593/Hx/Nx rats subjected to EVG staining. (Scale bar, 30 μm.) (*F*) Medial wall thickness index of rats in *E* (Veh/Hx/Nx: $n = 6$, SuHx: $n = 4$, Ki8751/Hx/Nx: $n = 3$, TAK-593/Hx/Nx: $n = 3$). (*G* and *H*) Percentages of open, partial, and closed pulmonary arteries with OD < 50 μm (*G*) and OD: 50–100 μm (*H*) of rats in *E* (Veh/Hx/Nx: $n = 6$, SuHx: $n = 4$, Ki8751/Hx/Nx: $n = 3$, TAK-593/Hx/Nx: $n = 3$). Values are means ± SD; $^{****}P < 0.0001$, $^{***}P < 0.001$, $^{**}P < 0.01$, $^{*}P < 0.05$.

lesions which are observed in the advanced stage, RNA-seq and ChIP-seq were performed using 8-wk lungs of SuHx rats (Figs. 7*A* and 6*B*). We identified 702 genes that were down-regulated in *Ahr*$^{-/-}$. Pathway analysis using these 702 AHR-dependent genes revealed up-regulation of genes involved in immune cell signaling (i.e., cytokine–cytokine receptor interaction, T cell receptor signaling pathway, and hematopoietic cell lineage) (Fig. 7 *B* and *D*). GO enrichment analysis using these 702 AHR-dependent genes revealed up-regulation of genes involved in immune cell accumulation (i.e., lymphocyte migration, T helper 17 type immune response, regulation of monocyte chemotaxis, positive regulation of T cell migration, and leukocyte adhesion to vascular endothelial cells) (Fig. 7 *C* and *D*), indicating that inflammatory cells such as Th17 cells and monocyte-derived macrophages accumulated in SuHx lungs due to AHR activation. Several of the inflammation-related and immune-related genes were directly up-regulated by AHR (Fig. 7*D*). Interestingly, we found *Il6* and *Tgfb1*, which have crucial roles for differentiation of Th17 cells from naive T cells (27, 37), were up-regulated in an AHR-dependent manner (Fig. 7 *D* and *E*). Because AHR is a regulator of Th17 cells (28, 38, 39) and directly up-regulates the expression of IL-21 (40), the key inflammatory cytokine for the pathogenesis of PAH (13), we coimmunostained SuHx rat lungs harvested at 8 wk with antibodies against CD4 and IL-21. CD4^{+} cells including CD4^{+}IL-21^{+} cells accumulated around remodeled arterioles in *Ahr*$^{+/+}$ rats (Fig. 7 *F* and *H*). In contrast, in *Ahr*$^{-/-}$ rats, particularly, CD4^{+}IL-21^{+} cells

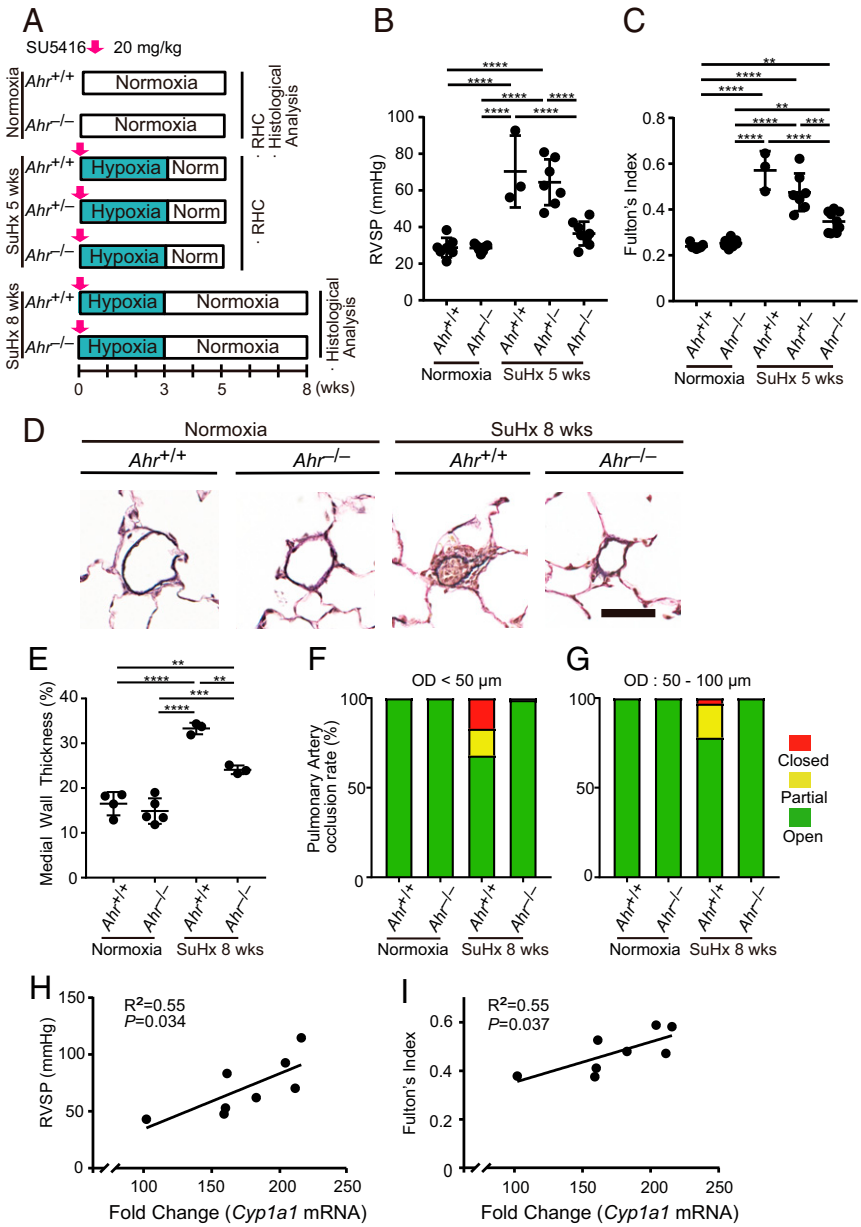

Fig. 4. *Ahr* $^{-/-}$ rats are resistant to PH in the SuHx rat model. (*A*) Experimental protocol for examining the role of the AHR signal pathway in the SuHx rat model. SU5416 or vehicle was subcutaneously administered to $Ahr^{+/+}$, $Ahr^{+/-}$, and $Ahr^{-/-}$ rats once on day 0. (*B* and *C*) Assessment of the SuHx model at 5 wk (normoxia $Ahr^{+/+}$: $n = 7$, normoxia $Ahr^{-/-}$: $n = 7$, SuHx 5-wk $Ahr^{+/+}$: $n = 3$, SuHx 5-wk $Ahr^{+/-}$: $n = 7$, SuHx 5-wk $Ahr^{-/-}$: $n = 8$). RVSP (*B*), Fulton's index (*C*). (*D*) Representative images of vascular remodeling of distal acinar arterioles in lung sections subjected to EVG staining in normoxia and SuHx 8-wk $Ahr^{+/+}$ or $Ahr^{-/-}$ rats. (Scale bar, 30 μm.) (*E*) Medial wall thickness index of SuHx 8-wk rats (normoxia $Ahr^{+/+}$: $n = 4$, normoxia $Ahr^{-/-}$: $n = 5$, SuHx 8-wk $Ahr^{+/+}$: $n = 3$, SuHx 8-wk $Ahr^{-/-}$: $n = 3$). (*F* and *G*) Percentages of open, partial, and closed pulmonary arteries of OD < 50 μm (*F*) and of OD: 50–100 μm (*G*) in SuHx 8-wk rats (normoxia $Ahr^{+/+}$: $n = 4$, normoxia $Ahr^{-/-}$: $n = 5$, SuHx 8-wk $Ahr^{+/+}$: $n = 3$, SuHx 8-wk $Ahr^{-/-}$: $n = 3$). (*H* and *I*) Relationships between RVSP and *Cyp1a1* mRNA levels (*H*) and between Fulton's index and *Cyp1a1* mRNA levels (*I*) in the lungs in SuHx 5-wk $Ahr^{+/+}$ rats. *Cyp1a1* mRNA levels are expressed as fold change relative to those of $Ahr^{+/+}$ rats' lung in normoxia. Values are means ± SD; $^{****}P < 0.0001$, $^{***}P < 0.001$, $^{**}P < 0.01$.

were rarely detected around arterioles (Fig. 7 *G* and *H*). CYP1A1 was expressed in subsets of $CD4^+$ cells in SuHx $Ahr^{+/+}$ rats (*SI Appendix*, Fig. S4*A*), but not in $Ahr^{-/-}$ rats (*SI Appendix*, Fig. S4*B*). These results suggest that AHR is involved in either proliferation or differentiation of Th17 cells during the pathogenesis of PAH and that the accumulation of Th17 cells partly contributes to the formation of advanced vascular lesions of SuHx PH.

Inflammatory Signals Are Activated in SuHx PBMCs in an AHR-Dependent Manner. To examine the relationship between AHR activation in immune cells and pathogenesis of PAH, we performed AHR-dependent gene expression profiling of peripheral blood mononuclear cells (PBMCs) from patients with Qing-Dai–induced PAH patients and SuHx rats (Fig. 8*A*). In PBMCs from both the PAH patients and SuHx rats, 52 genes were commonly up-regulated, including *CCL3, CCL2, IL1B, EGR1, EGR2, ATF3, PTGS2,* and *SOCS3* (Fig. 8*B* and *SI Appendix*, Fig. S5*A*); monocyte-related genes, including *CXCL11* and *CCR1*, were enriched (*SI Appendix*, Fig. S5*B*). Pathway analysis of genes up-regulated by Qing-Dai–induced PAH patients and SuHx rats revealed 12 common pathways related to inflammation, including NF-κB signaling, TNF signaling, and Toll-like receptor signaling (Fig. 8*C*). We previously reported that mannose receptor C-type lectin-1

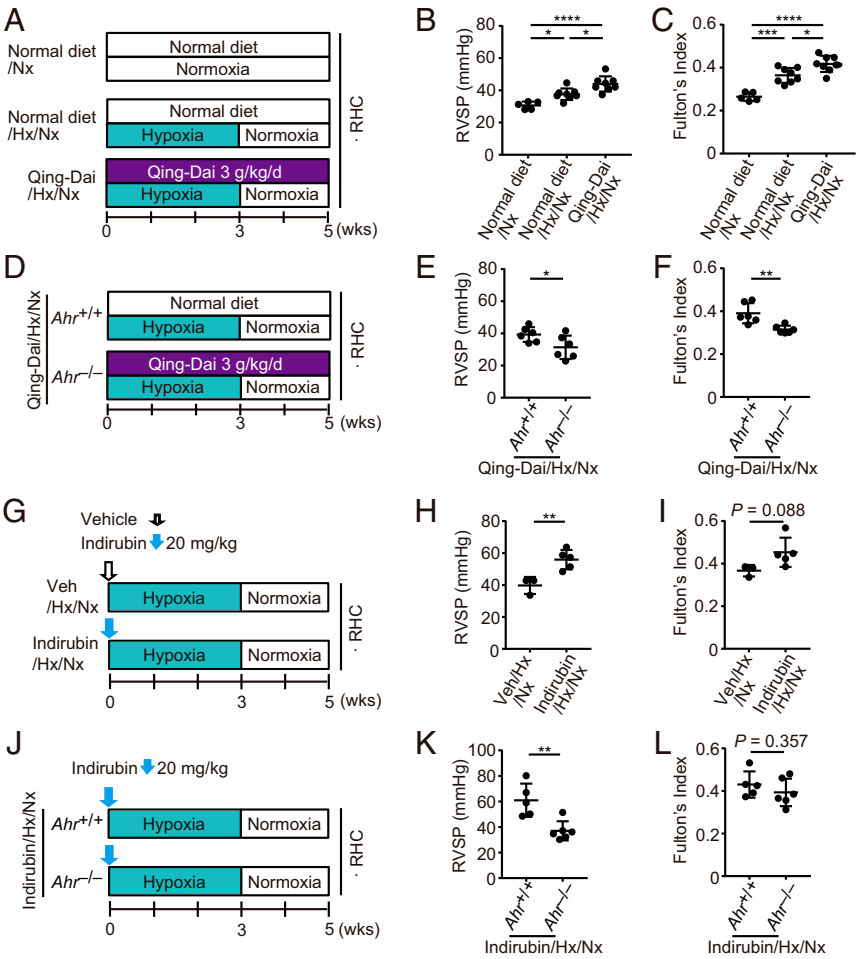

Fig. 5. Oral administration of Qing-Dai induces PH in rats in combination with hypoxia. (*A*) Experimental protocol for examining the effect of Qing-Dai–containing diet in combination with hypoxia on PH phenotype in rats (Qing-Dai/Hx/Nx rats). Qing-Dai–containing diet (3 g/kg/d) or control diet was fed to rats every day. (*B* and *C*) Assessment of Qing-Dai/Hx/Nx rats (normal diet/Nx: $n = 5$, normal diet/Hx/Nx: $n = 8$, Qing-Dai/Hx/Nx: $n = 8$). RVSP (*B*), Fulton's index (*C*). (*D*) Experimental protocol for examining the effect of *Ahr* deletion on Qing-Dai/Hx/Nx rats. Qing-Dai–containing diet (3 g/kg/d) was fed to $Ahr^{+/+}$ or $Ahr^{-/-}$ rats every day. (*E* and *F*) Assessment of the effect of *Ahr* deletion on the PH phenotype of Qing-Dai/Hx/Nx rats (Qing-Dai/Hx/Nx $Ahr^{+/+}$: $n = 6$, Qing-Dai/Hx/Nx $Ahr^{-/-}$: $n = 6$). RVSP (*E*), Fulton's index (*F*). (*G*) Experimental protocol for examining the effect of indirubin in combination with hypoxia (Indirubin/Hx/Nx rats). Indirubin or vehicle was subcutaneously administered once on day 0. (*H* and *I*) Assessment of Indirubin/Hx/Nx rats (Veh/Hx/Nx: $n = 3$, Indirubin/Hx/Nx: $n = 5$). RVSP (*H*), Fulton's index (*I*). (*J*) Experimental protocol for examining the effect of *Ahr* deletion on Indirubin/Hx/Nx rats. (*K* and *L*) Assessment of Indirubin/Hx/Nx rats (Indirubin/Hx/Nx $Ahr^{+/+}$: $n = 5$, Indirubin/Hx/Nx $Ahr^{-/-}$: $n = 6$). RVSP (*K*), Fulton's index (*L*). Values are means ± SD; $^{****}P < 0.0001$, $^{***}P < 0.001$, $^{**}P < 0.01$, $^{*}P < 0.05$.

$(MRC1)^+$ macrophages accumulated in vascular lesions in both patients with idiopathic pulmonary arterial hypertension (IPAH) who underwent lung transplantation and HPH mice (13). These findings strongly suggest that the accumulation of $MRC1^+$ macrophages into the vascular lesions of SuHx rats might be due to the infiltration of blood-borne monocytes. Hence, we analyzed the distribution of $MRC1^+$ macrophages in the lungs of SuHx rats. $MRC1^+$ macrophages accumulated around remodeled arterioles in $Ahr^{+/+}$ rats, but not in $Ahr^{-/-}$ rats (Fig. 8 *D* and *E*). These data suggest that inflammatory signals were AHR-dependently upregulated in PBMCs of both human PAH patients and SuHx rats and that $MRC1^+$ macrophages in PAH vascular lesions might be derived from PBMCs.

Activation of AHR in Endothelial and Bone Marrow-Derived Cells Induces PH in SuHx Rats. To assess whether AHR signaling of ECs or that of bone marrow (BM)–derived cells contributes to the pathogenesis of PH in the SuHx rat model, we performed bone marrow transplantation (BMT) experiments using $Ahr^{-/-}$ rats (Fig. 9 *A* and *B*). $Ahr^{-/-}$ recipients transplanted with $Ahr^{+/+}$ BM were significantly attenuated in PH phenotypes (Fig. 9 *C* and *D*), and $Ahr^{+/+}$ recipients transplanted with $Ahr^{-/-}$ BM were also attenuated to levels similar to those in $Ahr^{-/-}$ recipients transplanted with $Ahr^{-/-}$ BM (Fig. 9 *C* and *D*), indicating that AHR in both ECs and BM-derived cells is indispensable for PAH pathogenesis. To determine whether AHR activation is involved in the pathogenesis of human PAH, we performed immunostaining for AHR and CYP1A1. AHR accumulated in the nuclei in some ECs of acinar arteries, as well as in some leukocytes within or around acinar arteries (Fig. 9*E*). AHR accumulation was also observed in some cells within plexiform lesions (Fig. 9*E*). Presumably, as a consequence of AHR activation, CYP1A1 was also expressed in some ECs and infiltrating leukocyte-like cells in acinar arteries and plexiform lesions (Fig. 9*F*). These results suggest that AHR activation both in the ECs and in the immune cells of the lungs from IPAH patients is essential for the formation of PAH lesions (Fig. 9*G*).

Discussion

In this study, we showed that AHR-Luc activity in sera from PAH patients was higher than that from HV. We also demonstrated that activation of AHR is essential for the development

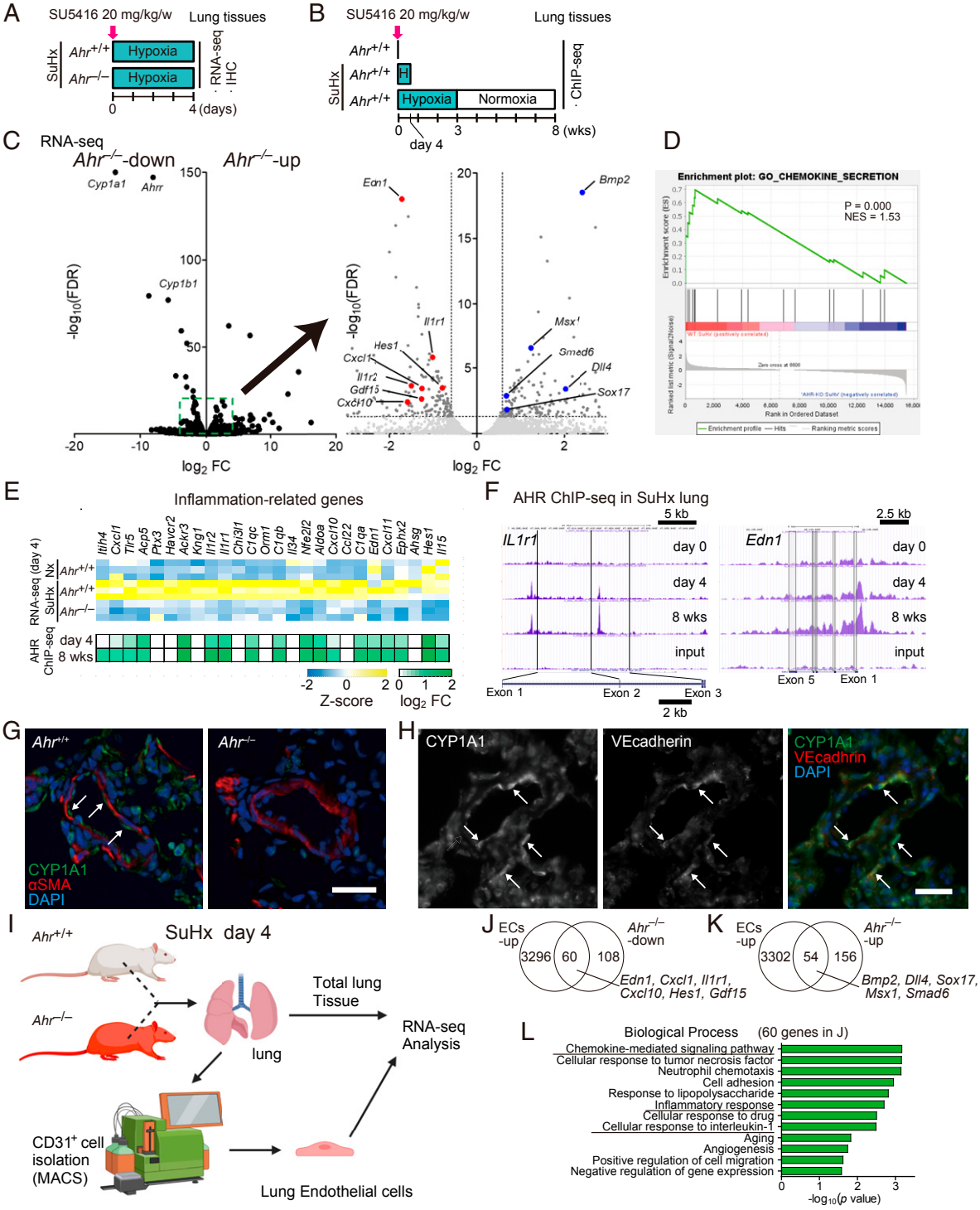

Fig. 6. Activation of AHR induces inflammation-related genes in endothelial cells of SuHx rats. (*A*) Experimental protocol for immunohistofluorescent analysis and RNA-seq analysis in the early stage (day 4) of SuHx rats. SU5416 was subcutaneously administered to $Ahr^{+/+}$ and $Ahr^{-/-}$ rats once on day 0 ($n = 3$ for each group). (*B*) Experimental protocol for ChIP-seq analysis of SuHx rats. SU5416 was subcutaneously administered to $Ahr^{+/+}$ rats once on day 0 ($n = 3$ pooled samples for each group). (*C*, *Left*) Volcano plot of AHR-dependent gene expression in SuHx rat lung on day 4. Typical AHR target genes are depicted in the plot. (*C*, *Right*) Enlarged diagram of the dashed box in the *Left*. PAH-related genes are depicted in the plot. (*D*) GSEA analysis of genes differentially expressed between $Ahr^{+/+}$ and $Ahr^{-/-}$ rats in the SuHx model with normalized *P* value and enrichment score (NES) for chemokine secretion. (*E*) Z-score of representative inflammation-related genes up-regulated in SuHx and AHR binding on these genes expressed as $\log_2$ fold change. (*F*) Representative ChIP-seq data of AHR in SuHx rat lung (days 0, 4, and 8 wk). (*G*) Representative immunofluorescence images of pulmonary arteries stained for CYP1A1 (green) and αSMA (red) in lung tissues of $Ahr^{+/+}$ (*Left*) and $Ahr^{-/-}$ (*Right*) on day 4 after SU5416 administration. Arrows indicate ECs. (Scale bar, 30 μm.) (*H*) Representative images of pulmonary arteries stained for CYP1A1 (*Left*) and VE-cadherin (*Middle*) in lung tissues of $Ahr^{+/+}$ SuHx rat on day 4; merged image is shown at *Right*. Arrows indicate representative cells double-stained for CYP1A1 and VE-cadherin. (Scale bar, 30 μm.) (*I*) Illustrative scheme of preparation of rat total lung tissue and $CD31^+$ ECs for RNA-seq analysis. (*J*) Venn diagram of genes up-regulated in ECs (ECs-up) and genes down-regulated in $Ahr^{-/-}$ ($Ahr^{-/-}$-down). (*K*) Venn diagram of ECs-up and genes up-regulated in $Ahr^{-/-}$ ($Ahr^{-/-}$-up). (*L*) GO enrichment analysis of the 60 genes indicated in *J*.

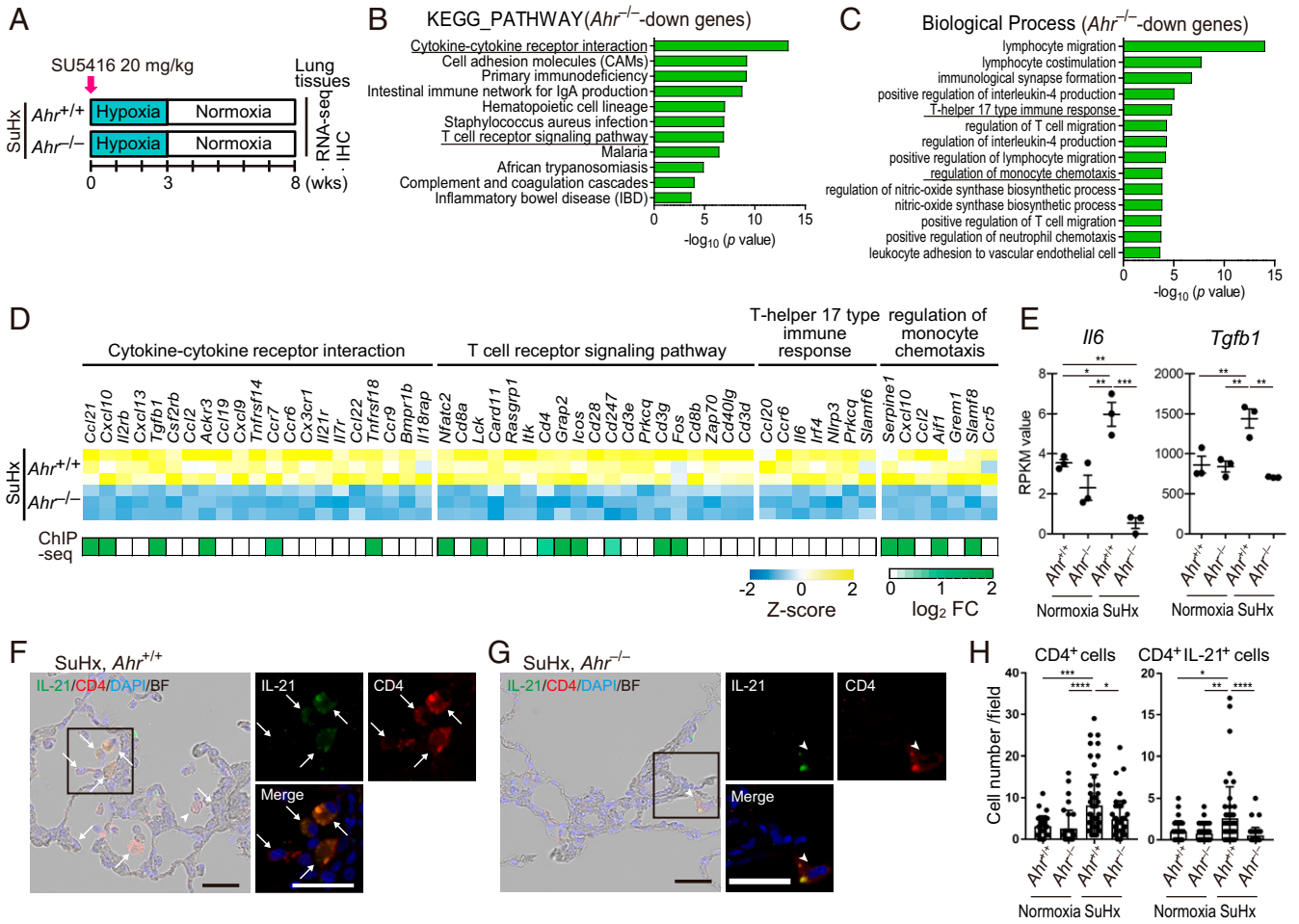

Fig. 7. AHR induces up-regulation of inflammatory signals and accumulation of $CD4^+IL\text{-}21^+$ T cells in vascular lesions in the advanced stage of SuHx rats. (*A*) Experimental protocol for RNA-seq ($n = 3$ for each group) and ChIP-seq ($n = 3$ pooled samples for each group) in the advanced stage of SuHx rats. SU5416 was subcutaneously administered to $Ahr^{+/+}$ and $Ahr^{-/-}$ rats once on day 0. (*B*) KEGG pathway enrichment analysis of 702 $Ahr^{-/-}$-down genes identified by RNA-seq analysis in SuHx rat lung at 8 wk. (*C*) GO enrichment analysis of the 702 genes. (*D*) Z-score of RNA-seq data and $\log_2$ fold change of enriched genes of ChIP-seq data about cytokine–cytokine receptor interaction, T cell receptor signaling pathway, T helper 17 type immune response, and regulation of monocyte chemotaxis in *B* and *C*. (*E*) RPKM values calculated in RNA-seq of representative genes about T helper 17 type immune response, *Il6* and *Tgfb1*. (*F*) Representative immunohistofluorescence images of pulmonary arterioles of SuHx 8-wk $Ahr^{+/+}$ rats stained for IL-21 and CD4. Arrows indicate cells double-positive for IL-21 and CD4 ($CD4^+IL\text{-}21^+$). Arrowheads indicate $CD4^+$ cells with attenuated expression of IL-21. (Scale bar, 30 μm.) (*G*) Representative immunohistofluorescence images of pulmonary arteries of SuHx 8-wk $Ahr^{-/-}$ rats stained with IL-21 and CD4. (*H*) Number of $CD4^+$ cells and $CD4^+IL\text{-}21^+$ cells of SuHx 8-wk $Ahr^{+/+}$ and $Ahr^{-/-}$ rats in 724 mm × 541 mm fields captured around arteries (number of tested rats: normoxia $Ahr^{+/+}$: $n = 3$, normoxia $Ahr^{-/-}$: $n = 3$, SuHx 8-wk $Ahr^{+/+}$: $n = 5$, SuHx 8-wk $Ahr^{-/-}$: $n = 4$). Values are means ± SD; $^{****}P < 0.0001$, $^{**}P < 0.01$, $^{*}P < 0.05$.

and progression of PAH. AHR was initially identified as a receptor for the environmental toxicant 2,3,7,8-tetrachlorodibenzo-p-dioxin (TCDD) (41, 42). Subsequent work showed that AHR signaling regulates various biological processes via activation of inflammatory signals in response to aromatic hydrocarbons from outside or inside the body (18, 19). On the basis of these findings, we propose that AHR plays a critical role as a regulator linking environmental cues to the pathogenesis of PAH.

Administration of the endogenous AHR agonist FICZ in combination with hypoxia (FICZ/Hx/Nx) induced severe PH with plexiform-like lesions, as seen in SuHx rats. The PH phenotypes observed in the SuHx and FICZ/Hx/Nx models were completely suppressed in $Ahr^{-/-}$ rats. These results indicate the importance of AHR signaling pathways both in the medial wall thickening and in the formation of intimal and plexiform-like lesions in PH rats. Consistent with our findings, AHR inhibitor partially inhibits PH phenotypes in SuHx rats (25). Despite the availability of many potent VEGFR2 inhibitors, no previous study has examined the effect of VEGFR2 inhibitors other than SU5416 on the induction of PH. In this study, administration of more potent VEGFR2 inhibitors in rats did not induce PH, even in combination with hypoxia. Taken together, these findings indicate that activation of AHR, but not inhibition of VEGFR2, plays an essential role in the pathogenesis of PH in the SuHx rat model.

Immunohistochemical analysis of SuHx rats and IPAH patients and BMT experiments of SuHx rats indicated that AHR expressed in both ECs and BM-derived cells is essential for the pathogenesis of PAH. RNA-seq analysis showed that AHR up-regulated a large number of inflammatory genes in lung vascular ECs of SuHx rats. ChIP-seq analysis revealed that AHR directly up-regulated many of these inflammatory genes; the canonical AHR-binding XRE motif (5′-CACGC-3′) as detected under most of the ChIP-seq peaks. Among these genes, we found several PAH-related genes such as *Edn1* and *Il1r1*. In the $Ahr^{-/-}$ rats, the medial wall thickening was attenuated in SuHx rats and

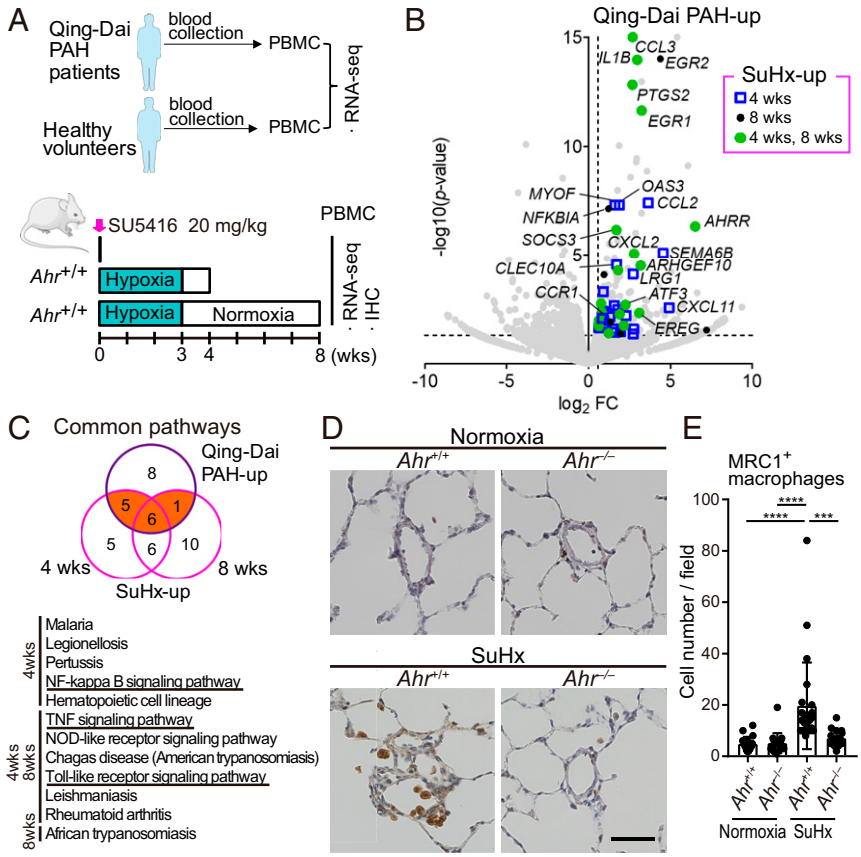

Fig. 8. Activation of AHR induces inflammation-related genes in PBMCs of SuHx rats and Qing-Dai–induced PAH. (*A*) Experimental protocol for RNA-seq of PBMCs in Qing-Dai–induced PAH patients ($n = 2$) and PBMCs in SuHx rat lungs ($n = 3$ for each group). (*B*) Volcano plot of gene expression of PBMCs in Qing-Dai–induced PAH patients vs. HV. Genes up-regulated in PBMCs of both patients and SuHx rats at 4 and 8 wk, identified by RNA-seq experiments, are indicated by blue open squares (4 wk), black circles (8 wk), and green circles (4 and 8 wk), respectively. (*C*) Pathway analysis of genes up-regulated by Qing-Dai and SuHx. Orange indicates the 12 common pathways, which are shown in the lower panel. (*D*) Representative immunohistochemical images of pulmonary arterioles stained for MRC1 in $Ahr^{+/+}$ and $Ahr^{-/-}$ rats. Arrows indicate $MRC1^+$ macrophages. (Scale bar, 50 μm.) (*E*) Number of $MRC1^+$ macrophages in 724 mm × 541 mm fields captured around arteries (number of tested rats: normoxia $Ahr^{+/+}$: $n = 3$, normoxia $Ahr^{-/-}$: $n = 3$, SuHx 8-wk $Ahr^{+/+}$: $n = 4$, SuHx 8-wk $Ahr^{-/-}$: $n = 3$). Values are means ± SD; $^{****}P < 0.0001$, $^{***}P < 0.001$.

our PH rats. Our immunohistochemical experiments showed that AHR is activated primarily in ECs, but not in smooth muscle cells, in SuHx rat lungs. These results suggest that activation of AHR in the ECs of pulmonary acinar arteries might secondarily affect medial wall thickening in SuHx rats.

Th17 cells ($CD4^+IL\text{-}21^+IL\text{-}17^+$ T cells) accumulated in the lung vascular lesions of HPH mice (13). In this study, pathway enrichment and immunohistochemical analyses revealed that $CD4^+IL\text{-}21^+$ T cells, presumably Th17 cells, accumulated in the lung vascular lesions of SuHx rats in an AHR-dependent manner. We previously reported that IL-6–dependent expression of AHR is crucial for the differentiation of Th17 cells, and AHR agonists promote Th17 cell differentiation induced by a combination of IL-6 and TGF-β (28, 29). In this study, the administration of FICZ induced severe PH only in a portion of the tested rats under normoxic conditions. In contrast, the administration of FICZ in combination with hypoxia induced severe PH in all of the tested rats. We also reported that hypoxia induces the up-regulation of IL-6 in the lungs, which induces the development of PH via induction of Th17 cells in HPH mice (13). Taken together, hypoxia might promote the AHR/Th17 axis by the production of inflammatory cytokines such as IL-6. Interestingly, *Il6* in SuHx rat lungs was up-regulated in an AHR-dependent manner in the advanced stage of SuHx rats, suggesting that activation of AHR could trigger a positive feedback loop of Th17 cell differentiation by the IL-6/AHR–signaling axis in PAH.

$MRC1^+$ macrophages, as well as $CD4^+IL\text{-}21^+$ T cells, were recruited to the vascular lesions of SuHx rats in an AHR-dependent manner. In our previous study, IL-21 blockade suppressed the accumulation of $MRC1^+$ macrophages to lesions in HPH mice (13). These findings suggest that IL-21 secreted from these $CD4^+IL\text{-}21^+$ cells might AHR-dependently recruit $MRC1^+$ macrophages around remodeled pulmonary arteries. The recruitment mechanisms of $CD4^+IL\text{-}21^+$ T cells and monocytes/macrophages into remodeled pulmonary arteries might be due to the interaction of chemokine–chemokine receptor signals expressed in lung ECs and blood monocytes. Macrophages recruited to small arteries in PH animal lungs contribute to pulmonary artery (PA) remodeling partly via the 5-lipoxygenase (5-LO)/leukotriene B4 (LTB4) signaling axis (43) and via the CXCL12-CXCR4–signaling axis (11, 13). AHR might therefore regulate these signaling axes to promote the PA remodeling in the PH rats in this study.

We showed that oral administration of Qing-Dai to rats recapitulated the PAH phenotype observed in refractory patients with UC treated with this drug. The phenotypes of Qing-Dai–induced PH were abolished in $Ahr^{-/-}$ rats, suggesting that AHR is responsible for this condition. In addition, we propose that indirubin is the causative compound for Qing-Dai–induced PAH. Indirubin is a compound contained in Qing-Dai that is a 50-fold more potent agonist of AHR than indigo (44). In addition to indirubin and indigo, Qing-Dai contains several other unknown substances (33). Future analyses of chemical composition of Qing-Dai may lead to identification of other

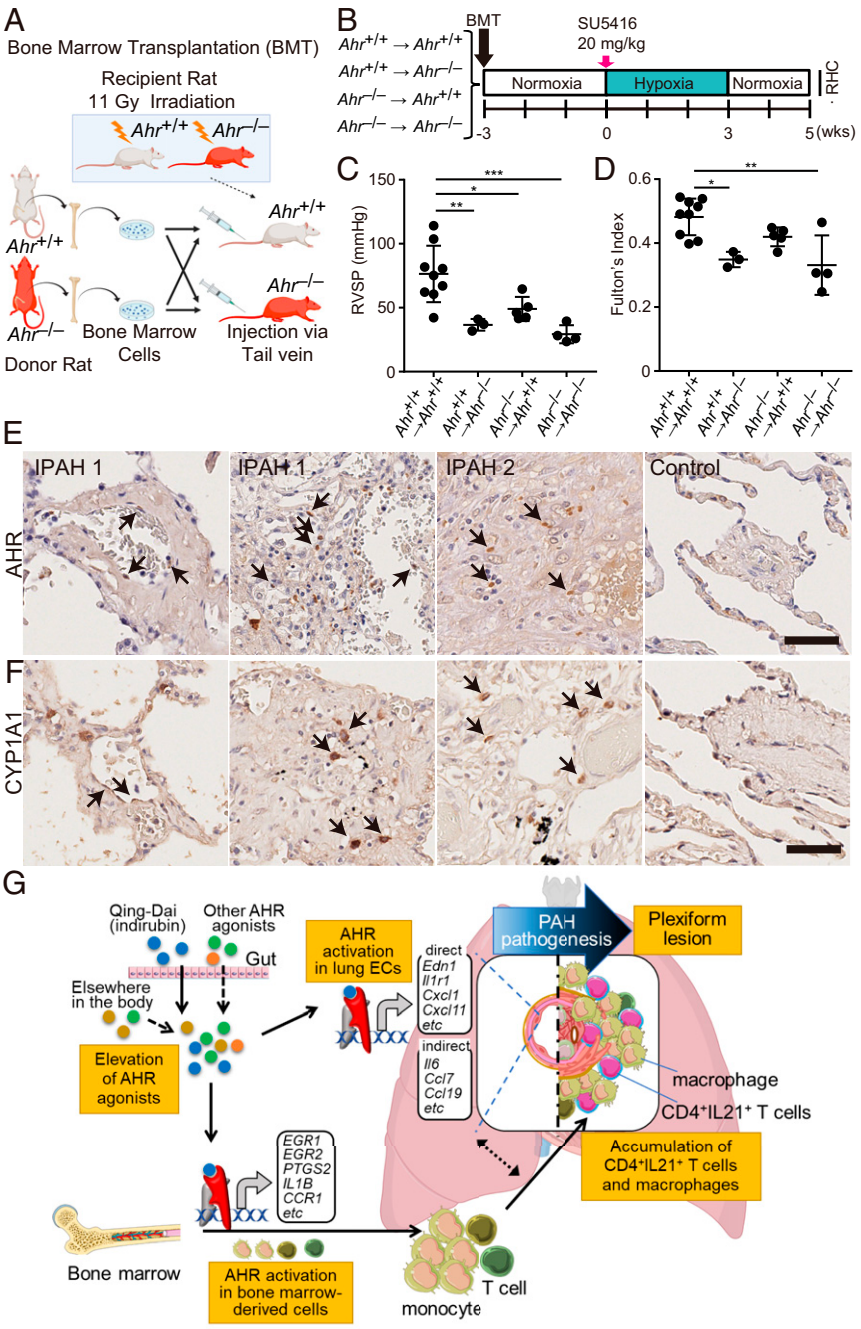

Fig. 9. The AHR signaling pathway both in ECs and in bone marrow-derived immune cells contributes to the pathogenesis of PAH. (*A*) Illustrative scheme of BMT experiment using $Ahr^{+/+}$ and $Ahr^{-/-}$ rats. $Ahr^{+/+}$ or $Ahr^{-/-}$ BM was transferred to $Ahr^{+/+}$ or $Ahr^{-/-}$ rats, respectively, after lethal irradiation (11 Gy). (*B*) Experimental protocol for RHC experiment for SuHx rats after BMT. Three weeks after BMT, SU5416 was subcutaneously administered to the rats. (*C* and *D*) Assessment of the SuHx rat model of BMT rats ($Ahr^{+/+}$ BM-transplanted $Ahr^{+/+}$: $n = 9$; $Ahr^{+/+}$ BM-transplanted $Ahr^{-/-}$: $n = 3$; $Ahr^{-/-}$ BM-transplanted $Ahr^{+/+}$: $n = 5$; $Ahr^{-/-}$ BM-transplanted $Ahr^{-/-}$; $n = 4$). RVSP (*C*), Fulton's index (*D*). (*E*) Representative images immunostained for AHR. Arrows indicate nuclear localization of AHR in ECs (IPAH 1, *Left*) and in infiltrating cells in a plexiform lesion (IPAH 1, right, and IPAH 2). No nuclear localization was seen around arteries in the control (Control). (*F*) Representative images immunostained for CYP1A1. Arrows indicate positive signals in some ECs (IPAH 1, *Left*) and in infiltrating cells in plexiform lesions (IPAH 1, right, and IPAH 2). No positive staining was seen around arteries in the control (Control). (Scale bar, 50 μm.) (*G*) Schematic illustration of development of PAH via AHR activation. This illustration was created using Servier Medical Art (https://smart.servier.com) and BioRender (https://biorender.com). Values are means ± SD; $***P < 0.001$, $**P < 0.01$, $*P < 0.05$.

AHR agonists involved in Qing-Dai–induced PAH. The low incidence of Qing-Dai–induced PAH (31) might be explained by either genetic background or by unknown environmental factors.

Here, we demonstrated that the AHR-Luc activity in sera was significantly higher in PAH patients than in HV and that the patients with higher AHR-Luc activity were significantly more susceptible to severe clinical events. These results indicate that AHR-Luc activity in the blood could serve as a prognostic marker for PAH. Sources of AHR agonists in the blood include diet, drugs, pollutants, metabolites of the gut microbiome, and

metabolites produced by the body. These environmental factors have been proposed to be involved in the pathogenesis of PAH (3, 4). Because AHR agonists have different potencies and efficacies for AHR activation, the AHR-Luc activity of the blood may depend on their total activities. These observations indicate that measurement of total AHR agonistic activity, i.e., AHR-Luc activity, in the blood is essential for the clinical assessment of PAH severity. Conventional therapies for PAH target three major pathways: the endothelin, nitric oxide, and prostacyclin pathways, all of which are involved in abnormal proliferation and contraction of the smooth muscle cells of the pulmonary artery. The advent of therapeutic agents targeting these pathways has dramatically improved the prognosis of patients with PAH (45). However, patients with severe PAH who are resistant to these medicines still have poor prognoses (46), and the development of therapeutic agents based on new drug targets is urgently required. Our results obtained in both animal models and human specimens indicate that inhibition of AHR signaling might prevent development of intimal lesions in severe patients with PAH (*SI Appendix*, Fig. S5*C*). On the basis of these findings, we propose that the AHR signaling pathway represents a promising therapeutic target.

In conclusion, we revealed that AHR signaling plays crucial roles in the development and progression of PAH and propose that AHR could be useful both as a therapeutic target and diagnostic marker for PAH.

Materials and Methods

Expanded methods for each subsection below are provided in *SI Appendix, Supporting Materials and Methods*.

Human Material and AHR Luciferase Reporter Assay. All protocols using human specimens were approved by the Institutional Review Board of the National Cerebral and Cardiovascular Center, Suita, Japan (M30-060, M30-168). AHR luciferase reporter assays were performed using the Human AhR Reporter Assay System (Indigo Biosciences). All patients and volunteers provided written consent for the use of their blood samples for biomedical research.

Animals. All experiments were carried out under the guidelines of the Animal Ethics Committee of the National Cerebral and Cardiovascular Center Research Institute and were also approved by the Institutional Review Board of the National Cerebral and Cardiovascular Center. Male Sprague–Dawley rats aged 6–9 wk (150–250 g) (Charles River Laboratories) were used in the animal experiments except for *SI Appendix*, Fig. S2 *E–G*. For *SI Appendix*, Fig. S2 *E–G*, female Sprague–Dawley rats aged 6–9 wk (150–200 g) were used. The *Ahr*$^{-/-}$ rat was created using CRISPR/Cas9 gene editing to delete exon 2; the knockout was produced at the Institute of Experimental Animal Sciences Faculty of Medicine, Osaka University.

Hemodynamic Measurements. During hemodynamic measurements, rats were anesthetized with isoflurane, and the trachea was cannulated for mechanical ventilation. An 18-gauge BD Angiocath catheter (Becton Dickinson) was inserted into the right jugular vein and advanced into the right ventricle to measure right ventricular pressure. Pressure signals were relayed to a BP Amp (ML117; AD Instruments). Data were acquired using the PowerLab data system (AD Instruments).

Statistical Analysis. All data are expressed as the means ± SD. Statistical analyses were performed using Graph Pad Prism 7 software. Comparisons of means between two groups were performed by unpaired Student's *t* test. Differences among multiple groups were compared by one-way ANOVA with post hoc Tukey–Kramer test. $P < 0.05$ was considered statistically significant.

Data Availability. Raw data of RNA-seq and ChIP-seq analysis of SuHx rats have been deposited in the National Center for Biotechnology Information Gene Expression Omnibus (GEO) database, https://www.ncbi.nlm.nih.gov/geo/ (accession no. GSE162245). All other study data are included in the article and supporting information.

ACKNOWLEDGMENTS. We thank Yuko Iwai and Nao Araki for secretarial assistance; Yasue Fukushima, Kazue Takei, and Noriko Maedera for technical assistance; and Manami Sone for technical assistance with histological analyses. We thank Tatsuo Aoki, Jin Ueda, and Akihiro Tsuji for collection and coordination of human blood samples. We thank Tomoji Mashimo and Yoshiki Miyasaka (the Institute of Experimental Animal Sciences Department of Medicine, Osaka University) for generating *Ahr*$^{-/-}$ rats. We thank Takeda Pharmaceutical Company for providing TAK-593. Computations were partially performed on the NIG supercomputer at ROIS National Institute of Genetics. This work was supported in part by Grants KAKENHI-16H05298 and 20H03682 (to Y.N.) and 20K08484 (to M.O.); the Intramural Research Fund (30-2-3) for Cardiovascular Diseases of National Cerebral and Cardiovascular Center; Practical Research Project for Rare/Intractable Diseases from Japan Agency for Medical Research and Development (AMED) (JP20ek0109415); Yakult Bio-Science Foundation; Takeda Science Foundation; Daiichi Sankyo Foundation of Life Science; Smoking Research Foundation; and Kishimoto Foundation (to Y.N.).

1. M. Humbert *et al*., Cellular and molecular pathobiology of pulmonary arterial hypertension. *J. Am. Coll. Cardiol.* **43**(12, suppl. S)13S–24S (2004).
2. M. Rabinovitch, Molecular pathogenesis of pulmonary arterial hypertension. *J. Clin. Invest.* **122**, 4306–4313 (2012).
3. M. Humbert *et al*., Pathology and pathobiology of pulmonary hypertension: State of the art and research perspectives. *Eur. Respir. J.* **53**, 1801887 (2019).
4. R. T. Schermuly, H. A. Ghofrani, M. R. Wilkins, F. Grimminger, Mechanisms of disease: Pulmonary arterial hypertension. *Nat. Rev. Cardiol.* **8**, 443–455 (2011).
5. D. Wu *et al*., Activation of aryl hydrocarbon receptor induces vascular inflammation and promotes atherosclerosis in apolipoprotein E-/- mice. *Arterioscler. Thromb. Vasc. Biol.* **31**, 1260–1267 (2011).
6. S. Kang, T. Tanaka, M. Narazaki, T. Kishimoto, Targeting interleukin-6 signaling in clinic. *Immunity* **50**, 1007–1023 (2019).
7. Y. Nakaoka *et al*., Efficacy and safety of tocilizumab in patients with refractory Takayasu arteritis: Results from a randomised, double-blind, placebo-controlled, phase 3 trial in Japan (the TAKT study). *Ann. Rheum. Dis.* **77**, 348–354 (2018).
8. M. Rabinovitch, C. Guignabert, M. Humbert, M. R. Nicolls, Inflammation and immunity in the pathogenesis of pulmonary arterial hypertension. *Circ. Res.* **115**, 165–175 (2014).
9. S. Yokota *et al*., Efficacy and safety of tocilizumab in patients with systemic-onset juvenile idiopathic arthritis: A randomised, double-blind, placebo-controlled, withdrawal phase III trial. *Lancet* **371**, 998–1006 (2008).
10. O. Takeuchi, S. Akira, Pattern recognition receptors and inflammation. *Cell* **140**, 805–820 (2010).
11. J. Bordenave *et al*., Neutralization of CXCL12 attenuates established pulmonary hypertension in rats. *Cardiovasc. Res.* **116**, 686–697 (2020).
12. H. Mori *et al*., Pristane/hypoxia (PriHx) mouse as a novel model of pulmonary hypertension reflecting inflammation and fibrosis. *Circ. J.* **84**, 1163–1172 (2020).
13. T. Hashimoto-Kataoka *et al*., Interleukin-6/interleukin-21 signaling axis is critical in the pathogenesis of pulmonary arterial hypertension. *Proc. Natl. Acad. Sci. U.S.A.* **112**, E2677–E2686 (2015).
14. M. N. Avilla, K. M. C. Malecki, M. E. Hahn, R. H. Wilson, C. A. Bradfield, The Ah receptor: Adaptive metabolism, ligand diversity, and the xenokine model. *Chem. Res. Toxicol.* **33**, 860–879 (2020).
15. C. Köhle, K. W. Bock, Coordinate regulation of Phase I and II xenobiotic metabolisms by the Ah receptor and Nrf2. *Biochem. Pharmacol.* **73**, 1853–1862 (2007).
16. T. Nakahama *et al*., Aryl hydrocarbon receptor deficiency in T cells suppresses the development of collagen-induced arthritis. *Proc. Natl. Acad. Sci. U.S.A.* **108**, 14222–14227 (2011).
17. C. H. Nguyen *et al*., Expression of aryl hydrocarbon receptor, inflammatory cytokines, and incidence of rheumatoid arthritis in Vietnamese dioxin-exposed people. *J. Immunotoxicol.* **14**, 196–203 (2017).
18. V. Rothhammer, F. J. Quintana, The aryl hydrocarbon receptor: An environmental sensor integrating immune responses in health and disease. *Nat. Rev. Immunol.* **19**, 184–197 (2019).
19. B. Stockinger, P. Di Meglio, M. Gialitakis, J. H. Duarte, The aryl hydrocarbon receptor: Multitasking in the immune system. *Annu. Rev. Immunol.* **32**, 403–432 (2014).
20. K. Abe *et al*., Formation of plexiform lesions in experimental severe pulmonary arterial hypertension. *Circulation* **121**, 2747–2754 (2010).
21. L. Taraseviciene-Stewart *et al*., Inhibition of the VEGF receptor 2 combined with chronic hypoxia causes cell death-dependent pulmonary endothelial cell proliferation and severe pulmonary hypertension. *FASEB J.* **15**, 427–438 (2001).
22. R. Tamosiuniene *et al*., Dominant role for regulatory T cells in protecting females against pulmonary hypertension. *Circ. Res.* **122**, 1689–1702 (2018).
23. T. A. Fong *et al*., SU5416 is a potent and selective inhibitor of the vascular endothelial growth factor receptor (Flk-1/KDR) that inhibits tyrosine kinase catalysis, tumor vascularization, and growth of multiple tumor types. *Cancer Res.* **59**, 99–106 (1999).
24. J. D. Mezrich *et al*., SU5416, a VEGF receptor inhibitor and ligand of the AHR, represents a new alternative for immunomodulation. *PLoS One* **7**, e44547 (2012).
25. A. Dean *et al*., Role of the aryl hydrocarbon receptor in sugen 5416-induced experimental pulmonary hypertension. *Am. J. Respir. Cell Mol. Biol.* **58**, 320–330 (2018).
26. G. Kwapiszewska, A. K. Z. Johansen, J. Gomez-Arroyo, N. F. Voelkel, Role of the aryl hydrocarbon receptor/ARNT/cytochrome P450 system in pulmonary vascular diseases. *Circ. Res.* **125**, 356–366 (2019).

27. A. Kimura, T. Naka, T. Kishimoto, IL-6-dependent and -independent pathways in the development of interleukin 17-producing T helper cells. *Proc. Natl. Acad. Sci. U.S.A.* **104**, 12099–12104 (2007).
28. A. Kimura, T. Naka, K. Nohara, Y. Fujii-Kuriyama, T. Kishimoto, Aryl hydrocarbon receptor regulates Stat1 activation and participates in the development of Th17 cells. *Proc. Natl. Acad. Sci. U.S.A.* **105**, 9721–9726 (2008).
29. T. Nakahama *et al*., Aryl hydrocarbon receptor-mediated induction of the microRNA-132/212 cluster promotes interleukin-17-producing T-helper cell differentiation. *Proc. Natl. Acad. Sci. U.S.A.* **110**, 11964–11969 (2013).
30. M. Nishio, K. Hirooka, Y. Doi, Chinese herbal drug natural indigo may cause pulmonary artery hypertension. *Eur. Heart J.* **37**, 1992 (2016).
31. M. Naganuma *et al*.; INDIGO survey Group, Adverse events in patients with ulcerative colitis treated with indigo naturalis: A Japanese nationwide survey. *J. Gastroenterol.* **54**, 891–896 (2019).
32. K. Misumi *et al*., Development of pulmonary arterial hypertension in a patient treated with Qing-Dai (Chinese herbal medicine). *Intern. Med.* **58**, 395–399 (2019).
33. I. Plitzko, T. Mohn, N. Sedlacek, M. Hamburger, Composition of indigo naturalis. *Planta Med.* **75**, 860–863 (2009).
34. K. Kubo *et al*., Novel potent orally active selective VEGFR-2 tyrosine kinase inhibitors: Synthesis, structure-activity relationships, and antitumor activities of N-phenyl-N′-4-(4-quinolyloxy)phenylureas. *J. Med. Chem.* **48**, 1359–1366 (2005).
35. N. Miyamoto *et al*., Discovery of N-[5-(2-[(cyclopropylcarbonyl)amino]imidazo[1,2-b] pyridazin-6-yloxy)-2-methylphenyl]-1,3-dimethyl-1H-pyrazole-5-carboxamide (TAK-593), a highly potent VEGFR2 kinase inhibitor. *Bioorg. Med. Chem.* **21**, 2333–2345 (2013).
36. J. A. Harrill *et al*., Knockout of the aryl hydrocarbon receptor results in distinct hepatic and renal phenotypes in rats and mice. *Toxicol. Appl. Pharmacol.* **272**, 503–518 (2013).
37. E. Bettelli *et al*., Reciprocal developmental pathways for the generation of pathogenic effector TH17 and regulatory T cells. *Nature* **441**, 235–238 (2006).
38. F. J. Quintana *et al*., Control of T(reg) and T(H)17 cell differentiation by the aryl hydrocarbon receptor. *Nature* **453**, 65–71 (2008).
39. M. Veldhoen *et al*., The aryl hydrocarbon receptor links TH17-cell-mediated autoimmunity to environmental toxins. *Nature* **453**, 106–109 (2008).
40. L. Apetoh *et al*., The aryl hydrocarbon receptor interacts with c-Maf to promote the differentiation of type 1 regulatory T cells induced by IL-27. *Nat. Immunol.* **11**, 854–861 (2010).
41. K. M. Burbach, A. Poland, C. A. Bradfield, Cloning of the Ah-receptor cDNA reveals a distinctive ligand-activated transcription factor. *Proc. Natl. Acad. Sci. U.S.A.* **89**, 8185–8189 (1992).
42. M. Ema *et al*., cDNA cloning and structure of mouse putative Ah receptor. *Biochem. Biophys. Res. Commun.* **184**, 246–253 (1992).
43. W. Tian *et al*., Blocking macrophage leukotriene b4 prevents endothelial injury and reverses pulmonary hypertension. *Sci. Transl. Med.* **5**, 200ra117 (2013).
44. L. Andrieux *et al*., Aryl hydrocarbon receptor activation and cytochrome P450 1A induction by the mitogen-activated protein kinase inhibitor U0126 in hepatocytes. *Mol. Pharmacol.* **65**, 934–943 (2004).
45. R. L. Benza *et al*., An evaluation of long-term survival from time of diagnosis in pulmonary arterial hypertension from the REVEAL Registry. *Chest* **142**, 448–456 (2012).
46. A. Ogawa, K. Ejiri, H. Matsubara, Long-term patient survival with idiopathic/heritable pulmonary arterial hypertension treated at a single center in Japan. *Life Sci.* **118**, 414–419 (2014).